Effect of Dissolved Carbon Dioxide on the Glass Transition and Crystallization of Poly(lactic acid) as Probed by Ultrasonic Measurements

J. Reignier, J. Tatibouët, R. Gendron

Industrial Materials Institute, National Research Council Canada, 75 de Mortagne Boulevard, Boucherville, Quebec, Canada J4B 6Y4

Received 1 October 2007; accepted 4 December 2007
DOI 10.1002/app.27896
Published online 5 February 2009 in Wiley InterScience (www.interscience.wiley.com).

ABSTRACT: The effects of dissolved carbon dioxide (CO_2) molecules on the glass-transition temperature as well as the crystallization kinetics of poly(lactic acid) have been investigated with a novel device that combines ultrasonic and volumetric measurements. Ultrasonic parameters such as the sound velocity are very sensitive to crystallization and can be used to monitor the crystallization kinetics. The glass-transition temperature has been found to decrease nonlinearly as the CO_2 concentration increases. The maximum in the crystallization rate has been found to increase with the addition of CO_2. © 2009 Wiley Periodicals, Inc. J Appl Polym Sci 112: 1345–1355, 2009

Key words: biopolymers; blowing agents; crystallization; glass transition

INTRODUCTION

Poly(lactic acid) (PLA) is a biodegradable polymer that can be made from renewable resources and has attracted enormous attention in the last decades because of its potential to replace conventional synthetic polymers for packaging applications. It is suitable for processes such as injection molding, blow molding, sheet extrusion, film forming, and even foam extrusion. One of the critical issues in PLA processing is the control of the crystallization kinetics and the degree of crystallinity of the final product. In general, the crystallization kinetics of PLA are slow enough to allow a quasi-amorphous sample to be prepared through quenching from the melt. It is worth noting that the lactide monomer used to produce PLA has two enantiomers, L and D. Control of the ratio of the L- and D-components is of critical importance because it has a large impact on the material properties. Thus, control of the composition, that is, the presence of D-lactide and *meso*-lactide, enables the generation of completely amorphous samples or samples with up to 40% crystalline structure with different crystallization kinetics. For instance, PLA with L-lactic acid content greater than 93% can be semicrystalline, whereas PLA with L-lactic acid content ranging from 50 to 93% is totally amorphous.

The presence of other species such as plasticizers can greatly affect polymer processing, particularly through a change in the crystallization behavior. Initially limited to rigid packaging applications, PLA has been blended with other polymers to circumvent the problem of brittle rupture and low plastic deformation at room temperature [glass-transition temperature (T_g) $\cong$ 50–60°C]. For instance, the addition of plasticizers such as poly(ethylene glycol) (PEG) into the amorphous phase of semicrystalline PLA was found not only to decrease T_g as expected but also to shift the crystallization event, observed during the heating of an amorphous film, to a lower temperature.[1] These effects were more pronounced with PEG of a low molecular weight and high PEG content. However, the crystallization level was found to decrease with the addition of PEG from 42% for neat PLA (D-lactide content of 4.1%) to 35% for the sample containing 10 wt % PEG during nonisothermal crystallization. On the other hand, other authors[2] have reported that the addition of PEG greatly promotes the crystallization level up to about a 36% crystalline fraction for 90/10 PLA/PEG blends, whereas neat PLA (8% D-lactide units) is only weakly crystallized with less than about a 0.5% crystalline fraction. Caution should be paid to these results because they have been obtained under nonisothermal conditions. Isothermal crystallization experiments showed that the addition of plasticizers increased the spherulite growth rate from 0.46 μm/

Correspondence to: J. Tatibouët (jacques.tatibouet@imi.cnrc-nrc.gc.ca).

min for neat PLA to 1.6 μm/min for a sample containing 10 wt % PEG at a crystallization temperature (T_c) of 130°C.[1] In the same way, Hobbs and Barham[3] observed at the ambient temperature a 14-fold increase in the crystal growth rate (radial expansion) of films of poly(hydroxybutyrate), which is also a biodegradable polyester, like PLA, upon the addition of water.

The crystallization of PLA in the presence of other polymer molecules has been the subject of intensive study in the last decade. However, much less is known about the effect of more volatile molecules such as carbon dioxide (CO_2) on the crystallization of PLA, despite the importance of kinetics in predicting crystallization during polymer processing. Studies on the influence of dissolved gas on T_g and the crystallization kinetics of the polymer are much more difficult because of the high volatility of the gas, but they are of critical importance for foam processing. Ohshima's group, using a high-pressure differential scanning calorimeter, has produced interesting results for various polymer/CO_2 systems. In that case, the calorimetric measurements were made with the sample chamber surrounded by pressurized CO_2. In the case of poly(ethylene terephthalate) (PET), Takada and Ohshima[4] demonstrated that the presence of CO_2 increased the overall crystallization rate of PET, whatever the isothermal T_c was. In a previous study on polypropylene (PP),[5] they observed that the dissolved CO_2 reduced the overall crystallization rate within the nucleation-dominated temperature region, that is, in the high T_c range. In the case of PLA, Takada et al.[6] demonstrated that the crystallization rate was accelerated by the presence of CO_2 molecules in the crystal-growth-controlled region, whereas it was depressed in the nucleation-controlled region. They also demonstrated that the crystallization rate followed the Avrami equation, with Avrami coefficient (n) values varying between 1.63 and 2, depending on the value of T_c and the CO_2 pressure. For comparison, Sato et al.[7] reported a value of n close to unity for a CO_2 pressure of 5 MPa but a value of 2.4 for intermediate pressures ranging between 2.5 and 3 MPa, with this last value being closer to those obtained by Takada and coworkers. The latter also reported from the same study that the presence of CO_2 did not change the crystalline structure for CO_2 pressures up to 2 MPa, as evidenced by analysis of wide-angle X-ray diffraction patterns. However, the proportion of the crystalline phase at the end of the crystallization event was found to increase with the pressure level of CO_2. For instance, it increased from about 26% for the neat PLA to more than 45% for a CO_2 saturation pressure of 2 MPa and a T_c value of 140°C. All these results suggest one-dimensional rodlike growth for a high CO_2 pressure (5 MPa) but two-dimensional disclike and three-dimensional spherulitic growth for a CO_2 pressure below 3 MPa.

Thus, reports on the effect of dissolved CO_2 on the crystallization rate of different polymers can be quite different. According to Takada and coworkers,[4,6] these different behaviors may be explained by the competition between the depression in the equilibrium melting temperature (T_m^0) and T_g. It is well accepted that the crystallization rate changes with the isothermal T_c value according to a bell-shaped curve. The maximum crystallization rate occurs at a given temperature called T_c^{max}, which was found to be nearly equal to the mean of T_g and T_m^0, that is, $T_c^{max} = (T_g + T_m^0)/2$. In the low T_c region ($T_g < T_c < T_c^{max}$), the crystallinity is controlled by the crystal growth rate or diffusion because of the increasing thermodynamic driving force with increasing undercooling ($\Delta T = T_m - T_c$, where T_m is the melting temperature) and the decreasing chain mobility at a lower temperature. On the opposite, in the high T_c region ($T_c^{max} < T_c < T_m$), the crystallization kinetics are controlled by the nucleation rate, which is significantly reduced because of the lower undercooling and the higher mobility of the polymeric chains.

Thus, a crystallization model has been proposed to describe the dependence of the crystallization rate on the temperature:[8,9]

$$\ln k = C_1 - \frac{C_2 T}{\left(T - T_g + C_3\right)^2} - \frac{C_4 T_m^0}{T\left(T_m^0 - T\right)} \quad (1)$$

where k is the parameter of crystallization kinetics for the nucleation and growth rate, whereas C_i (i = 1 to 4) represents constants that have to be determined by the fitting of eq. (1) to the experimental crystallization data. Using the same approach of Ito et al.[9] to take into account the pressure effects on T_g and T_m^0, Takada and Ohshima[4] extended this model to incorporate the effect of CO_2 on the crystallization kinetics by introducing a linear dependence of T_g and T_m^0 on CO_2 pressure [P_{CO_2}] into eq. (1):

$$T_g = T_{g,\text{nitrogen}} - \alpha P_{CO_2} \quad (2)$$

$$T_m^0 = T_{m,\text{nitrogen}}^0 - \beta P_{CO_2} \quad (3)$$

where α and β are constants. According to the hypothesis that the depression in T_m is almost the same as the depression in T_m^0, the magnitude of change of T_g and T_m under pressurized CO_2 should control the evolution of k. If $\alpha \sim \beta$, then the crystallization rate is accelerated in the crystal-growth-controlled region, but it is depressed in the nucleation-controlled region, as is the case for the PP/CO_2 system.[6] However, if $\alpha \gg \beta$, then the crystallization rate is increased by CO_2 dissolution over the whole

T_c range, such as in the PET/CO_2 system.[4] Even if the enhancement of the mobility of the polymeric chains due to the presence of dissolved gas is claimed to be the major factor acting on the crystallization behavior of the polymer/gas mixture, which promotes crystallization at a lower temperature, it appears from all that has been discussed that the crystallization curve [ln $k = f(T)$] is not only shifted to a lower temperature in the presence of a plasticizer but also can be displaced upward or downward, that is, along the crystallization rate axis.

Unfortunately, the use of a high-pressure differential scanning calorimeter does not allow us to separate the effect of pressure from that of the concentration of dissolved gas molecules in the polymer sample because the latter is pressure-dependent. Therefore, the true effects of hydrostatic pressure on T_m and T_c and on the crystallization rate are not generally taken specifically into account. T_m and T_c generally increase with pressure. For example, in the case of pure poly(L-lactide acid), Nakafuku[10] reported a pressure (P) dependence of T_m (dT_m/dP) of 0.173 K/MPa under nonisothermal conditions.

Therefore, to determine quantitatively the respective influence of the hydrostatic pressure and dissolved CO_2 content on the crystallization kinetics, a novel technique was used in this work. This technique is based on the ultrasonic characteristics (velocity and attenuation) and volumetric measurements performed under controlled pressure and temperature conditions. These variables are very sensitive to the structural properties of the material. This original technique was therefore very useful in discriminating the effects of the pressure and concentration of dissolved gas on crystallization because the concentration of CO_2 was set once before the ultrasonic characterization and accordingly was independent of the hydrostatic pressure applied during the measurements. In addition to the effect of dissolved CO_2 on the crystallization of PLA, the plasticization of PLA by CO_2 was also probed with this same unique device. Moreover, experiments were conducted under isothermal conditions. Finally, the ultrasonic results were compared to those derived from volumetric measurements.

EXPERIMENTAL

Materials

Two PLA resins, grades 8302D and 2002D, were both purchased from NatureWorks (Minnetonka, MA). According to the supplier, grade 8302D (coded PLA1 in this work) is a completely amorphous copolymer with a D-content of 9.85 wt % and a number-average molecular weight around 80,000, whereas grade 2002D (coded PLA2) is semicrystalline with a D-content of 4.25 wt % and a number-average molecular weight of 90,000. According to the supplier's information, no nucleating agent was added to the semicrystalline materials. Both materials were dried for around 8 h at 50°C before the experiments. Commercial-grade CO_2 was used without any further purification.

Differential scanning calorimetry (DSC)

DSC experiments were carried out on neat PLA2 (without CO_2) in a DSC Q1000 apparatus (TA Instruments, New Castle, DE). Specimens were first heated up to 200°C and maintained at that temperature for 10 min to ensure complete melting of the crystalline phase, and then they were cooled at a rate of −40°C/min to the selected T_c. Sufficient time was allowed to complete the crystallization stage ($\sim$ 12 h), after which the samples were cooled to 0°C at −40°C/min. After cooling, a subsequent heating scan at 10°C/min was performed to determine the crystallinity level of the sample. Because of the thermal degradation of PLA at high temperatures, a different sample was used for each T_c experiment.

Ultrasonic measurements

Experiments were carried out with a unique device previously developed in our laboratory, which is described in detail elsewhere.[11] Basically, ultrasonic characterization of materials is based on the propagation characteristics (sound velocity and attenuation) of small-amplitude, high-frequency waves (typically 2.5 MHz in our case) through a sample. Monitoring the ultrasonic parameters has been found to be very efficient for investigating crystallization phenomena, especially when pressure is applied or when gas or a foaming agent is dissolved in the material.[12–14] In addition, the device allows monitoring of the thickness of the sample by the use of a linear variable differential transformer transducer and hence gives access to the specific volume.

Experiments were performed on cylindrical samples (32 mm in diameter and 3 mm thick) that were molded from pellets directly into the sample holder of the ultrasonic measurement system under 20 MPa and at 200°C for about 10 min. For crystallization experiments without CO_2, the sample was then quickly cooled to the desired T_c value at a constant pressure.

An investigation of the effect of CO_2 on the crystallization of PLA requires the dissolution of CO_2 in the PLA matrix. For that purpose, some of the molded samples, obtained from quenching under the aforementioned molding conditions, were placed in a pressure vessel (Parr reactor) filled with CO_2 and maintained at room temperature for 24 h with various saturation pressures. After pressure release, the sample was quickly transferred to the ultrasonic

measurement device, in which a pressure of 30 MPa was rapidly applied to prevent undesired foaming or gas loss. With this pressure maintained, the temperature was increased up to 200°C, then the pressure was adjusted to 20 MPa, and the sample was quickly cooled to T_c. An accurate concentration of CO_2 in the PLA sample was later determined by the weighing of the sample before and after final degassing outside the device in a vacuum oven.

Because of the sample handling performed under atmospheric conditions, part of the CO_2 may have diffused out of the sample before weighing. To address this issue, the following procedure was conducted. The initial weight of the sample, that is, immediately after pressure release and device opening, which corresponded then to the composition of the material during the experiments, was obtained by extrapolation at time zero of the decreasing weight as a function of time. The percentage error in the CO_2 content due to the diffusivity issue was thus estimated to a value of 0.05 wt %, this small number being explained by the relatively thick (3-mm) geometry of the sample and the very low diffusion coefficient of CO_2 in PLA (10^{-12} to 10^{-11} m^2/s)[15] under such conditions.

Evaluation of the crystallization kinetics

The crystallization kinetics were evaluated on the basis of Avrami's general theory with the well-known double-logarithmic form:

$$\log_{10}[-\ln(1 - X_t)] = \log_{10} k + n \log_{10} t \qquad (4)$$

where n is the Avrami exponent, which reflects the geometry of crystal growth and the mechanism of nucleation, and k represents the overall kinetic rate constant. As usual, the time required to reach 50% crystallization (relative) is called the half-time of crystallization ($t_{1/2}$). This latter parameter is used to compare the crystallization kinetics. It was estimated from k and n with the following relation:

$$t_{1/2} = [(\ln\ 2)/k]^{1/n} \qquad (5)$$

RESULTS AND DISCUSSION

Effect of the pressure on the ultrasonic characteristics of semicrystalline PLA

Before we considered the effect of dissolved CO_2 on the glass-transition and crystallization behaviors, PLA2 samples were first ultrasonically characterized at various pressures ranging from 5 to 60 MPa. The purpose of these preliminary experiments, in addition to observing the effect of applied pressure on the various parameters, was to evaluate if the PLA samples would crystallize during cooling from the molten state at the various pressures investigated.

Figure 1 gives the evolution of the ultrasonic velocity and attenuation as well as the specific volume of PLA during cooling from 200 to 30°C at a rate of −2°C/min for different applied pressures. The breakpoint on the specific volume curve (as indicated by the black arrow) corresponds to T_g of PLA. T_g obtained from the specific volume measurements was found to increase linearly with pressure with a slope of 0.26°C/MPa, as shown in Figure 2.

The consequences of crystallization on the ultrasonic parameters (attenuation and velocity) are well documented because various semicrystalline polymers have been thoroughly investigated previously.[12–14,16] The ultrasonic behavior of PLA2 during the cooling run did not show any features corresponding to the crystallization of the material in the investigated range of pressures. No evidence of crystallization, referring to the volumetric behavior, was found either. These results are, however, not surprising because the crystallization of PLA is known to be very slow.

The attenuation spectrum is characterized by the existence of a single relaxation peak (α relaxation) related to the glass-transition phenomena.[16] As a result of the pressure dependence of T_g, this symmetrical relaxation peak is shifted toward higher temperatures when pressure is increased, as displayed in Figure 1(a). For comparison, the temperature of the peak maximum (T_{max}) is plotted in Figure 2 as a function of the applied pressure.

S-shaped curves, as depicted in Figure 1(b), are the results of plotting the velocity as a function of temperature. As for attenuation, velocity curves are shifted toward a higher temperature when the pressure is increased.

Effect of dissolved CO_2 on T_g of completely amorphous PLA

Representative plots of the attenuation for completely amorphous PLA1 samples are shown in Figure 3 for temperature sweeps between 200 and −50°C (during cooling) and at various concentrations of CO_2. This figure illustrates a well-known result: the presence of dissolved CO_2, which increases free volume, affects the mobility of the polymer chains, as a plasticizer usually does. This results in significant shifts of the α-relaxation peak to lower temperatures. For instance, the peak maximum shifts from 110 to about 45°C when 10 wt % CO_2 is dissolved in PLA, and this indicates the strong plasticization imparted to the material by CO_2. Similar effects have been reported in the case of biodegradable polyesters such as poly(ε-caprolactone) with dissolved CO_2.[13]

Figure 4(a) presents the evolution of T_{max} as a function of the CO_2 content. The T_{max} decrease becomes nonlinear when the concentration of CO_2 is

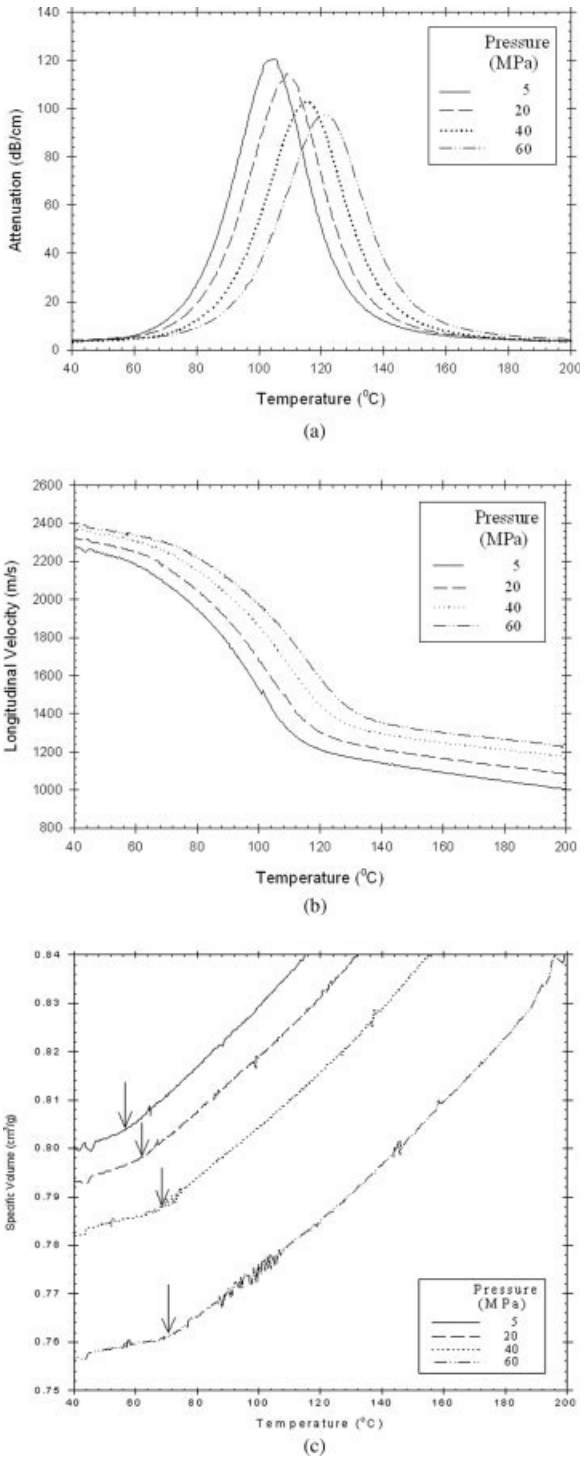

Figure 1 Evolution of (a) the attenuation, (b) sound velocity, and (c) specific volume as a function of temperature for PLA1 with various applied pressures: (—) 5, (- - -) 20, (· · ·) 40, and (- · -) 60 MPa. The samples were first heated at 200°C and then cooled to the ambient temperature at a rate of −2°C/min. The breakpoints on the specific volume curve area, indicated by the black arrows, correspond to T_g.

increased beyond about 10 wt %. Another interesting characteristic of the relaxation peak is its surface area (A_α), which can be related to the relaxation intensity. The evolution of A_α with the CO_2 content is reported in Figure 4(b). A_α does not change significantly for concentrations lower than 5 wt % CO_2, and this means that a larger peak width compensates for a smaller height in this concentration range. The peak area decrease becomes important at higher CO_2 concentrations. In fact, polymer relaxation experiments (frequency sweeps) have demonstrated that the height of the damping peaks, the loss factor being proportional to the product of the attenuation by the ultrasonic velocity, is roughly inversely proportional to the width of the peak.[17] The model used by Hartmann et al.[17] to fit the experimental data was based on the Havriliak–Negami equation, which adopts a reminiscent form of the well-known time–temperature principle. In other words, increasing the

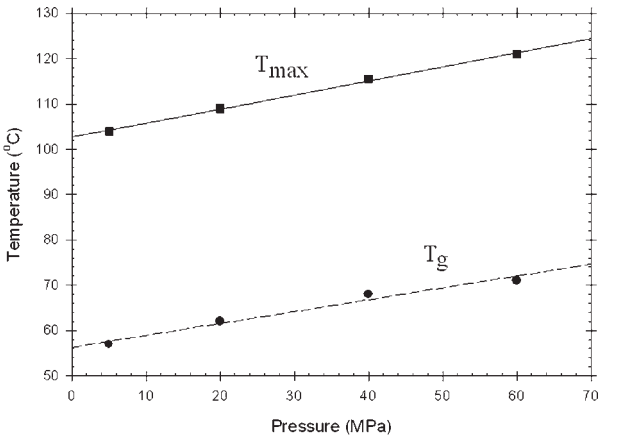

Figure 2 Evolution of T_g obtained from the breakpoint in the specific volume curve and T_{max} obtained from the attenuation curve as a function of the applied pressure for PLA1.

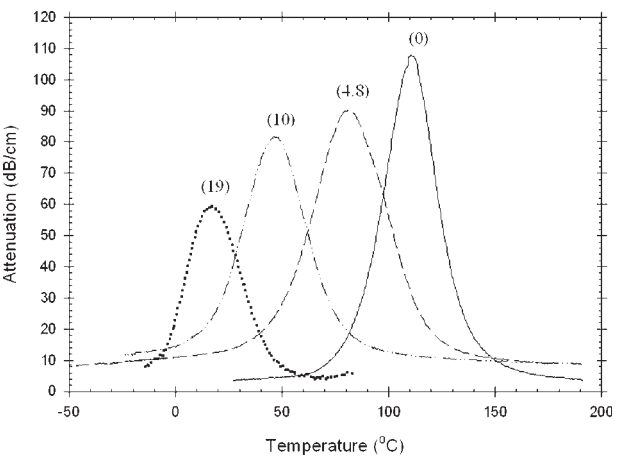

Figure 3 Evolution of the attenuation of PLA1 (100% amorphous) during a temperature sweep from 200 to −60°C with various CO_2 contents. The numbers in parentheses above each relaxation peak correspond to the concentrations of CO_2 (wt %) in the samples. The pressure was maintained at 20 MPa throughout each experiment.

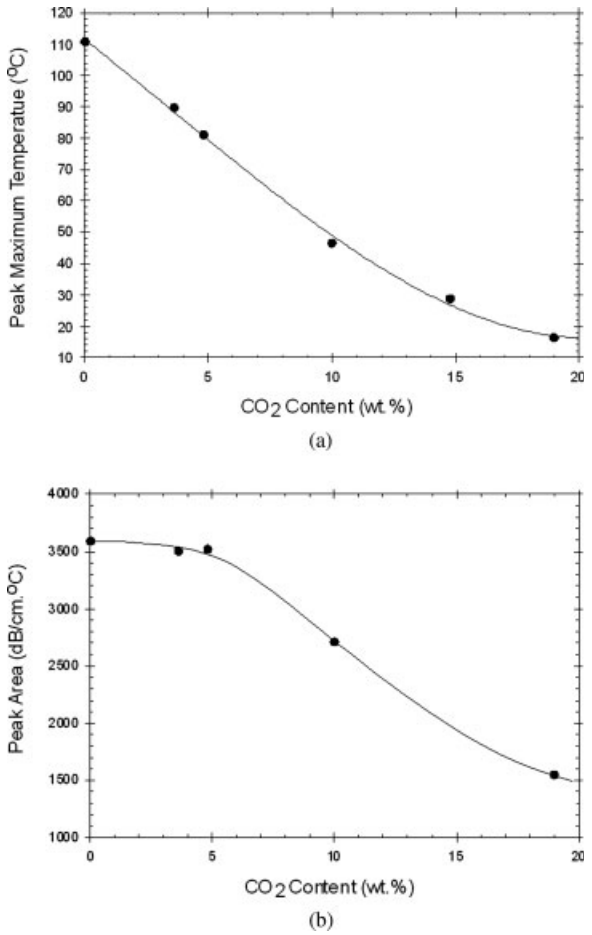

Figure 4 Evolution of (a) the relaxation peak maximum temperature and (b) the relaxation peak area observed in the attenuation curve as a function of the CO_2 content for PLA1. The lines are only guides for the eyes.

frequency will have the same effect as a decrease in temperature. In our case, the frequency of the ultrasonic wave was fixed at a constant value of about 2.5 MHz, but the addition of CO_2, which plasticized the PLA matrix, can be seen as a change in frequency because of the time–temperature superposition principle. It would thus be expected that the integrated surface area of the relaxation peak should not change significantly with the concentration of CO_2, despite the change in the height and width of the relaxation peak. However, as can be seen in Figure 4(b), A_α drops abruptly beyond 5 wt % CO_2, thus indicating that a particular phenomenon is occurring at a higher CO_2 content. The decrease in A_α may be explained by the decrease in the number of relaxing chains or, more likely, by the decrease in the energy that dissipated during relaxation. In that latter case, a possible explanation would be that intermolecular and/or intramolecular interactions of PLA chains become weaker because of the high concentration of CO_2. Aside from the swelling effect that implies an increase in the free volume, the presence of CO_2 in a high concentration may lubricate the polymeric chains and leads to the decrease in the reptation time of the PLA molecules. This critical CO_2 concentration corresponds also to the increase in the crystallinity and to the important enhancement of the nucleation rate observed in batch foaming experiments.[18]

One of the critical point is to determine to what extent T_g is depressed upon the addition of CO_2 molecules. Figure 5 summarizes the T_g depression of PLA as a function of the CO_2 weight content, as determined from the breakpoint in the specific volume during cooling and the estimation from a model developed by Chow.[19] Chow proposed a theoretical relation to estimate the depression of T_g caused by absorption of dissolved small molecules. Mainly based on the respective molecular weight of the diluent and the polymer repeat unit, the evolution of T_g is described as follows:

$$\ln\frac{T_g}{T_{g0}} = \psi[(1-\theta)\ln(1-\theta) + \theta\ln\theta] \tag{6}$$

$$\theta = \frac{\omega/M_d}{z(1-\omega)/M_p} \tag{7}$$

$$\psi = \frac{zR}{M_p\Delta C_p} \tag{8}$$

where T_{g0} is the glass-transition temperature for the pure polymer and T_g is the value for a given weight fraction (ω) of the diluent. M_d and M_p are the molecular weights of the diluent and polymer repeat unit, respectively. ΔC_p is the change in the specific heat of the polymer at its T_g, and R is the gas constant. The

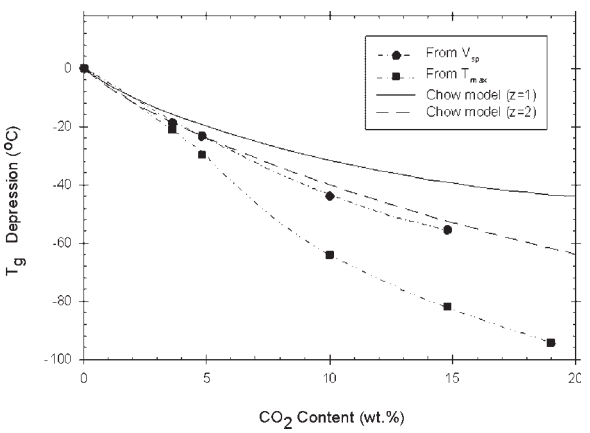

Figure 5 Depression in T_g estimated with various methods as a function of the CO_2 content for PLA1. Experimental points were obtained either by ultrasonic measurements (T_{max} in the attenuation signal) or by volumetric measurements [breakpoint in the specific volume (V_{sp}) curve]. The Chow model was used for comparison with different values of z. Dotted lines are only guides for the eyes.

parameters for the PLA/CO_2 system used in the calculations were M_d = 44 g/mol, M_p = 72 g/mol, ΔC_p = 0.548 J/g/K, and T_{g0} = 328.3 K. The lattice coordinate number (z) was alternatively set equal to 1 and 2 for comparison. This z number represents the number of macromolecules in contact with a single CO_2 molecule.[20] However, from a practical point of view, z may be used as a fitting parameter that enables us to take into account molecular interactions. The value of z corresponding to the best fit with experimental results was found to be dependent on the nature of the polymer.

Comparing our experimental results with Chow's predictions in Figure 5, we find from this plot that the ΔT_g–CO_2 content relation derived from the Chow model with z = 1 underestimates the experimental points obtained from volumetric measurements. However, the T_g depression curve estimated from the model with z = 2 seems to be able to accurately estimate the experimental points obtained from the breakpoint in the specific volume.

Because the effects of applied pressure on T_g and T_{max} depressions are related, it is interesting to wonder whether the T_g depression upon CO_2 absorption could also be evaluated from the shift in T_{max}. At a low CO_2 content, typically below 5 wt % CO_2, the ΔT_{max} curve seems to closely match the T_g depression obtained from the specific volume. However, for CO_2 contents greater than about 5 wt %, the T_g depression obtained from T_{max} overestimates the depression in T_g. For instance, the discrepancy with the model is around 20°C for 10 wt % CO_2.

Isothermal crystallization of PLA2

Effect of CO_2 on the crystallization kinetics as probed by ultrasonic and volumetric characteristics

The isothermal crystallization of PLA2 was examined in detail with our ultrasonic device coupled with volumetric measurements, with or without the presence of dissolved CO_2. The results corresponding to the unplasticized PLA2 (without CO_2) are compared with results obtained more classically by DSC measurements in the next section.

Our analysis begins with the evolution of the ultrasonic characteristics and specific volume as a function of time, as shown in Figure 6 for PLA/3.9 wt % CO_2 for different isothermal T_c values. The data corresponding to the evolution with temperature during cooling to T_c are not reported. However, it is worth noting that in all cases, no crystallization of the PLA sample occurs during that cooling step (−2°C/min) down to T_c, whereas it was expected that the presence of CO_2 might accelerate the crystallization kinetics. The crystal formation during the cooling ramp would have been accompanied by an abrupt change in the attenuation signal, which was not the case.

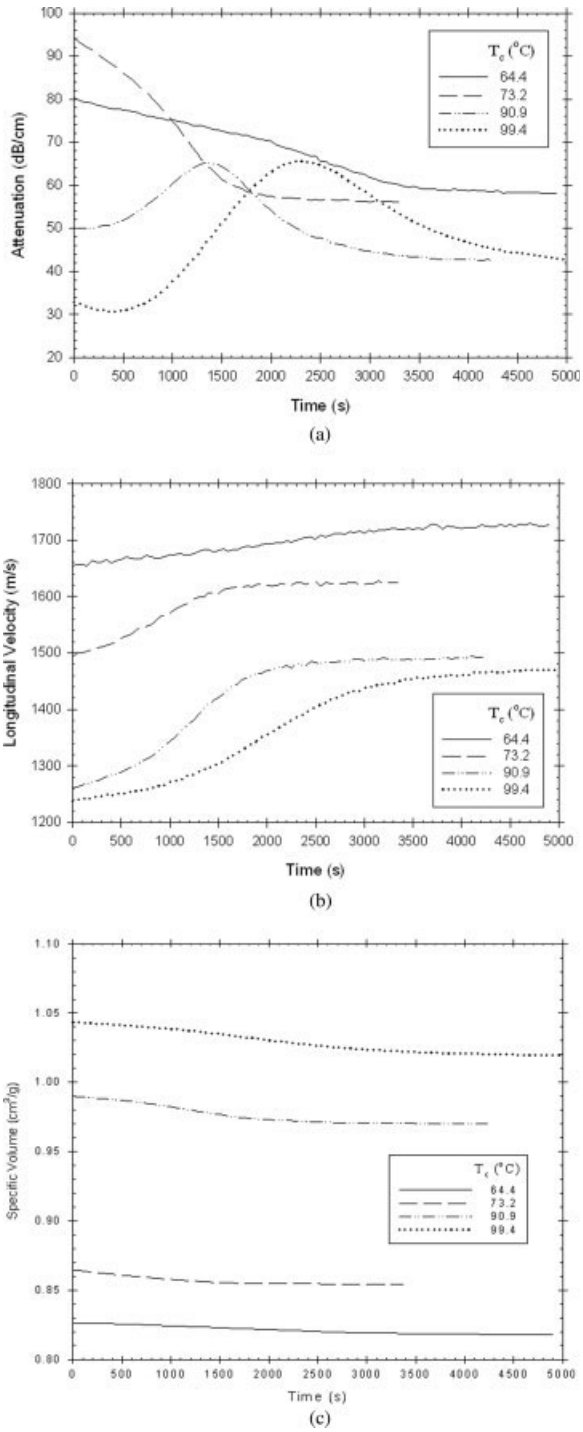

Figure 6 Variation of (a) the attenuation, (b) ultrasonic velocity, and (c) specific volume during isothermal crystallization induced at various temperatures for PLA2/3.9 wt % CO_2 as a function of time. The initial time corresponds to the beginning of the isothermal plateau.

The time of crystallization in an Avrami plot is usually regarded as the time interval from the instant (t = 0) when T_c is attained. However, in our case, it is difficult to determine the start time

because of the temperature rate decrease at the end of the cooling ramp. The onset of crystallization (t = 0) was precisely chosen as the point at which the specific volume drops abruptly (breakpoint) on a plot of the specific volume versus the temperature. Surprisingly at first, the shape of the attenuation curve with time during isothermal crystallization varies quite a lot from one T_c to the other. However, it has to be kept in mind that the starting point on the relaxation curve is not the same, and thus the effect of crystal formation on signal attenuation may be quite different. For T_c lower than T_{max}, which is about 75°C in the case of PLA2/3.9 wt % CO_2 [Fig. 6(a)], attenuation decreases continuously because of the reduction of the proportion of the amorphous phase during crystallization. On the contrary, for T_c greater than 75°C, the crystallization event is characterized by a peak (as a function of time), the maximum of which should correspond to the onset of percolation of crystallites.[16] Therefore, because of the complex dependence of the attenuation signal on the temperature and crystalline morphology, as shown in Figure 6(a), crystallization kinetics cannot be investigated with the absolute attenuation as a parameter.

On the other hand, the ultrasonic speed and specific volume both show a nice sigmoidal curve ended by a plateau. In addition, both the beginning of the velocity increase and leveling off at the plateau coincide with the change in the specific volume. Similarly to the classical approach developed by the combination of DSC measurements and Avrami's model, it has been shown in the past[13] that the relative crystallinity or fractional crystallinity [$X_c(t)$] can also be defined by the variation of the specific volume through the replacement of the exothermic enthalpy with the specific volume:

$$X_c(t) = \frac{V_0 - V_t}{V_0 - V_\infty} = 1 - \exp\left(-kt^n\right) \qquad (9)$$

where V_0 is the initial specific volume and V_t and V_∞ are the specific volumes at time t and at the final plateau, respectively. k is the crystallization constant, and n is the Avrami exponent, as usual. Similarly, it is obvious to wonder whether the ultrasonic velocity can also be used to estimate $X_c(t)$ and hence the various kinetic crystallization parameters according to the following relation:

$$X_c(t) = \frac{v_t - v_0}{v_\infty - v_0} = 1 - \exp\left(-kt^n\right) \qquad (10)$$

where v_0 is the initial longitudinal velocity and v_t and v_∞ are the longitudinal velocities at time t and at the final plateau, respectively. Again, k is the crystallization constant, and n is the Avrami exponent. Interestingly, the variation of the velocity as a function of time is quite large, and this seems to indicate that this parameter is very sensitive to crystal formation and could therefore be used to easily follow the crystallization kinetics. On the contrary, variations in the specific volume during crystallization are rather small, and the beginning of the final plateau corresponding to the end of crystallization is barely detectable with good accuracy; this is mainly due to the small difference in the specific volume of the pure PLA crystal with respect to completely amorphous PLA (difference in the specific volume $\sim$ 0.023 cm^3/g at room temperature and normal pressure).[21] Nevertheless, both approaches were used to investigate the difference in the crystallization kinetics for the neat PLA (without CO_2) and PLA/3.9 wt % CO_2 system according to Avrami's model. Conventionally with DSC, $t_{1/2}$ corresponds to the time at which half the area under the isothermal crystallization peak has been generated. This specific approach can be extended to eqs. (9) and (10) if we take the time corresponding to X_c = 0.5. Even though $t_{1/2}$ emphasizes the early stage of crystal formation, which is much more related to the nucleation stage, compared to the later stage of crystal growth, which is more affected by chain mobility, we decided to compare the crystallization kinetics of PLA2 with or without CO_2 by investigating $t_{1/2}$.

The results for PLA with and without CO_2 are summarized on Figure 7, in which the $t_{1/2}$ values

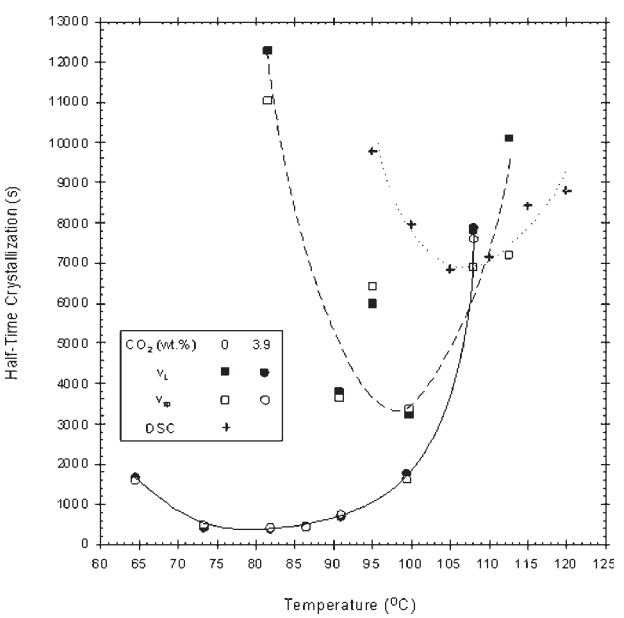

Figure 7 Effect of the CO_2 content on $t_{1/2}$ of PLA2 as a function of temperature under various pressure conditions. Values of $t_{1/2}$ were determined either under atmospheric pressure by DSC (crossed symbols) or under a pressure of 20 MPa by ultrasonic velocity (v_L) measurements (solid symbols) and by specific volume (v_{sp}) measurements (open symbols). Lines are only guides for the eyes.

issued from both specific volume and sound velocity variations are plotted as a function of the crystallizing temperatures. Three significant results have been observed.

First, as shown in Figure 7, the results for $t_{1/2}$ obtained from the variation in the ultrasonic velocity compare very well with those obtained from the volumetric change for samples with or without CO_2. Usually, the determination of crystallization kinetics is obtained from volumetric or enthalpic measurements. Up to now, the use of ultrasonic measurements was restricted to the determination of the T_c and T_m values of various polymers,[12,16] but the results displayed in Figure 7 clearly show that the ultrasonic velocity can also be used with success to evaluate the $t_{1/2}$ values.

Second, the differences in $t_{1/2}$ curves shown in Figure 7 for neat PLA and PLA/3.9 wt % CO_2 clearly illustrate the influence of CO_2 on the crystallization behavior. For instance, $t_{1/2}$ at $T_c \sim 82°C$ for the sample containing dissolved CO_2 is more than 1 order less than that for the sample without CO_2. It should be remembered that the hydrostatic pressure applied to the sample is the same in both cases (20 MPa), and thus the difference between the two curves is strictly related to the presence of CO_2.

Third, Figure 7 seems also to indicate that CO_2 has the tendency to flatten the dependence of $t_{1/2} = f(T_c)$ at the bottom of the curve, that is, for temperatures below 100°C. The minimum in $t_{1/2}$ (maximum crystallization rate) can be considered almost constant over a wider temperature range in the presence of CO_2 than for the CO_2-free PLA sample.

It has been shown in the past that crystallization (isothermal conditions) is accelerated by high pressure.[9] For that purpose, it was decided to investigate the crystallization kinetics of neat PLA2 with classical DSC experiments. For the DSC runs, the onset of crystallization ($t = 0$) was chosen as the point at which the exothermic peak starts. As the heat of fusion of PLA is found in the literature with typical values ranging from 65 to 140 J/g, the crystallization kinetics were determined by the calculation of X_c at time t as the ratio of the area under the heat flow curve at t to the total area of the peak. The $t_{1/2}$ values have been determined and are plotted as a function of temperature in Figure 7. Comparisons with the values obtained by ultrasonic and volumetric measurements for an isostatic pressure of 20 MPa show clearly a decrease in $t_{1/2}$. The minimum in $t_{1/2}$, corresponding to the temperature at which the crystallization rate is maximum, is shifted toward a low temperature when pressure is applied.

Figure 8 illustrates the effect of CO_2 on the evolution of $X_c(t)$ as a function of time for $T_c \sim 100°C$. The presence of CO_2 shifts the S-shaped curve to smaller times, and that unambiguously indicates an

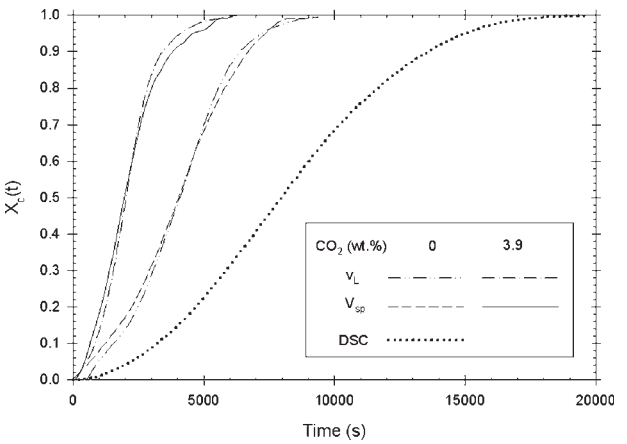

Figure 8 Variation of $X_c(t)$ as a function of time for $T_c = 100°C$. Values of $X_c(t)$ obtained by ultrasonic, volumetric, and enthalpic measurements are reported on the same plot for comparison (v_L = ultrasonic velocity; V_{sp} = specific volume).

acceleration of the crystallization kinetics in this temperature range (self-diffusion-controlled region). When the PLA/CO_2 system is isothermally crystallized at a temperature lower than about 105°C, CO_2 enhances the ability of PLA to crystallize (small $t_{1/2}$). On the other hand, CO_2 slows the crystallization kinetics at higher T_c values. Takada et al.[6] demonstrated, using high-pressure DSC and another grade of semicrystalline PLA, that the crystallization rate was accelerated by CO_2 at $T_c < 130°C$ (self-diffusion-controlled region) and depressed at higher T_c (nucleation-controlled region). Despite differences between temperature limits for the two regions, similar tendencies have been observed in our case with a completely different characterization technique. As mentioned in the introduction, two factors can affect the crystallization rate of semicrystalline polymers in the presence of CO_2. First, adding CO_2 reduces both T_m and T_m^0 and thus reduces the driving force for crystallization ($T_m^0 - T_c$). In addition, the dissolution of CO_2 into the polymeric material lowers T_g of the amorphous matrix through an increase of the segmental mobility of the macromolecules. In the particular case of PLA, it thus appears that the magnitude of the depression in T_g induced by the presence of dissolved CO_2 is almost the same as the depression in T_m^0.

The effect of pressure is also demonstrated in Figure 8, in which the time evolution of $X_c(t)$ is displayed for ultrasonic, volumetric, and enthalpic measurements. The effect of pressure is obviously visible.

At this point of the discussion, it is interesting to remember that all the aforementioned results are based on the relative (or fractional) crystallinity because the absolute crystallinity is unknown and may change from one T_c to the other and with the

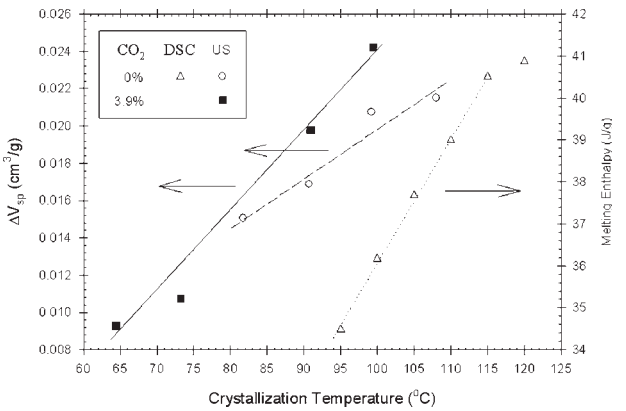

Figure 9 Evolution of the crystallinity as probed by (a) the variation in the specific volume (ΔV_{sp}) during isothermal crystallization (left axis) obtained from the ultrasonic device (US) and (b) the melting enthalpy (right axis) measured after isothermal crystallization with DSC. The lines are only guides for the eyes. Open symbols correspond to neat PLA2, whereas filled symbols correspond to PLA2 with 3.9 wt % CO_2. DSC experiments were conducted under atmospheric pressure, whereas the isostatic pressure in the US was maintained at 20 MPa.

presence of CO_2. For that purpose, some authors have modified eq. (9) to take into account the true crystalline fraction (absolute value with respect to the amorphous content):

$$X_c = 1 - \exp\left(-\frac{1}{X'}\frac{\rho_c}{\rho_l}kt^n\right) \tag{11}$$

where X_∞ is the crystalline fraction (absolute) at the end of the crystallization and ρ_c and ρ_l are the densities of the crystalline and liquid phase, respectively. Unfortunately, the precise determination of ρ_c and ρ_l is quite difficult, even impossible—they depend not only on the temperature but especially on the presence of CO_2—and hence an estimation of the crystallinity with these inaccurate values would be inappropriate. Nevertheless, the variation of the crystalline fraction can be estimated at least qualitatively by the variation in the specific volume, before and after completion of crystallization, as shown in Figure 9 for the different T_c values investigated. The increase in the variation of the specific volume for neat PLA and PLA/3.9 wt % CO_2 seems to indicate that the proportion of the crystalline phase at the end of the crystallization event increases with T_c. Interestingly, the dependence (slope) of the variation of the specific volume as a function of T_c is slightly greater in the case of the PLA/CO_2 system with respect to neat PLA. Similar trends have been shown by Takada et al.[6] in the case of PLA with a more pronounced effect at high T_c. However, the absolute value of the variation of the specific volume and hence absolute crystallinity cannot be compared for the different systems studied.

The evolution of the melting enthalpy with T_c is also shown in Figure 9 for the DSC runs. The increase of the crystalline fraction with T_c is demonstrated in Figure 9, in which the melting enthalpy is shown to increase slightly with T_c. Assuming a fusion enthalpy of 81 J/g for 100% crystalline PLA,[22] the crystalline level was found to increase from 42 to 49% as T_c increased from 95 to 115°C.

Estimate of parameter n

We estimated the crystallization parameter n by plotting $\log_{10}[-\ln(1 - X_c)]$ values versus $\log_{10} t$ and taking the slope around $t_{1/2}$. Figure 10 gives an example of Avrami's plot for the PLA/3.9 wt % CO_2 system at three different temperatures; the evolution of $X_c(t)$ was obtained from the velocity measurements. The values of n derived from the ultrasonic velocity and specific volume are reported in Table I. Values for n obtained by DSC are summarized in Table I. They indicate that the variation in the ultrasonic velocity is in relatively good agreement with the more classical determinations based on volumetric measurements and is independent of the presence of CO_2. Values of n are almost constant over the range of T_c values, within the experimental error, and can be compared to values deduced from DSC experiments in the case of the neat material.

The small discrepancies between the n values determined either by volumetric or velocity measurements can be explained as follows. As mentioned previously, the ultrasonic velocity is highly sensitive to the crystal formation, whereas the change in the specific volume is quite small. As a result, the choice

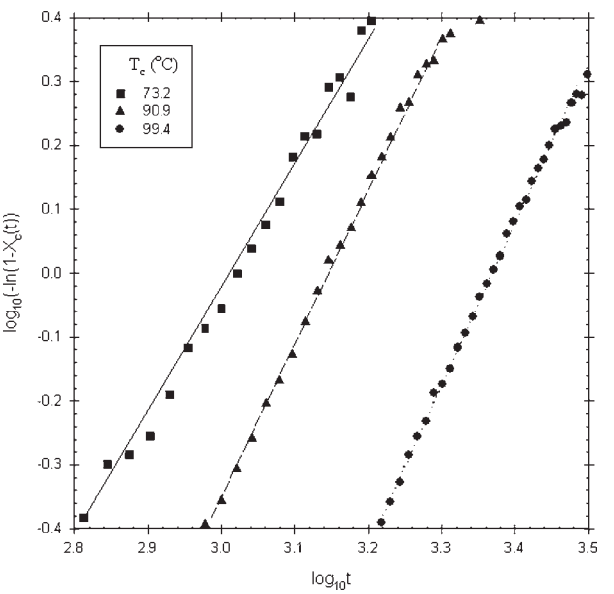

Figure 10 Avrami's log–log plots for PLA2/3.9 wt % CO_2 for various T_c values.

TABLE I
Results for n as Determined with Different Techniques for the Various Conditions Investigated (T_c and CO_2 Content)

	n				
	No CO_2		3.9 wt % CO_2		Nitrogen
T_c (°C)	V_{sp}	v_L	V_{sp}	v_L	atmosphere (DSC)
64.4			1.9	2.2	
73.2			1.3	1.6	
81.7	2.0	2.4			
90.7	2.1	2.7			
90.9			2.0	2.4	
95					2.2
99.2	2.2	2.2			
99.4			2.0	2.5	
100					2.1
105					2.2
108	2.1	2.9			
110					1.8
120					1.7

v_L = ultrasonic velocity; V_{sp} = specific volume.

of the value of the ultrasonic velocity at the beginning of the crystallization event ($t = 0$) is more critical because of this higher sensitivity.

CONCLUSIONS

The effect of dissolved CO_2 on T_g and the crystallization kinetics of PLA was investigated with an original device combining ultrasonic and volumetric measurements. Ultrasonic propagation parameters such as the sound velocity and attenuation are sensitive to the structural state of the material and can be used easily to study the CO_2-induced depression in T_g and to monitor the crystallization kinetics with or without CO_2.

The depression in T_g was found to decrease nonlinearly with the CO_2 content according to Chow's law with $z = 2$. The α relaxation was investigated through attenuation measurements, indicating that the energy that dissipates during relaxation is strongly reduced beyond 5 wt % CO_2. A possible explanation is the weakening of intermolecular and intramolecular interactions of PLA chains because of the high CO_2 concentration.

Sound velocity and attenuation are very sensitive to the crystallization of PLA. The crystallization rate in the presence of CO_2 was found to increase essentially in the self-diffusion-controlled regions. The results issued from velocity measurements can be favorably compared to the volumetric change method in determining $t_{1/2}$ and n in an Avrami analysis of the crystallization. The results differ from those obtained by DSC measurement for neat PLA at normal pressure.

Moreover, the ultrasonic method allows the discrimination between CO_2 concentration effects and pure pressure effects by opposition to the pressurized DSC measurements. The ultrasonic method can also probe the material under experimental conditions that are closer to those existing during classical foam extrusion.

Although the concentration of CO_2 investigated in this work was set to 3.9 wt %, a choice made to mimic conditions representative of those used in foam extrusion of PLA, it would be worthwhile to extend such a study to a broader range of CO_2 contents. Such additional works are currently progressing.

References

1. Kulinski, Z.; Piokowska, E. Polymer 2005, 46, 10290.
2. Pillin, L.; Montrelay, N.; Grohens, Y. Polymer 2006, 47, 4676.
3. Hobbs, J. K.; Barham, P. J. Polymer 1997, 38, 3879.
4. Takada, M.; Ohshima, M. Polym Eng Sci 2003, 43, 479.
5. Takada, M.; Tanigaki, M.; Ohshima, M. Polym Eng Sci 2001, 41, 1938.
6. Takada, M.; Hasegawa, S.; Ohshima, M. Polym Eng Sci 2004, 44, 186.
7. Sato, Y.; Takeuchi, K.; Takishima, S.; Masuoka, H. Polym-Supercrit Fluid Syst Foams 2003, 83, 2993.
8. Ishizuka, O.; Koyama, K. Polymer 1977, 18, 913.
9. Ito, H.; Tsutsumi, Y.; Minagawa, K.; Takimoto, J.; Koyama, K. Colloid Polym Sci 1995, 273, 811.
10. Nakafuku, C. Polym J 1994, 26, 680.
11. Piché, L.; Massines, F.; Hamel, A.; Néron, C. U.S. Pat. 4,754,645 (1988).
12. Tatibouët, J.; Piché, L. Polymer 1991, 32, 3147.
13. Reignier, J.; Tatibouët, J.; Gendron, R. Polymer 2006, 47, 5012.
14. Liegey, F.; Tatibouët, J.; Derdouri, A. Proc Soc Plast Eng Annu Tech Conf 2004, 1300.
15. Sato, Y.; Yamane, M.; Sorakubo, A.; Takishima, S.; Masuoka, H.; Yamamoto, H.; Takasugi, M. Jpn Symp Thermophys Prop 2000, 21, 196.
16. Piché, L. IEEE Ultrason Symp 1989, 599.
17. Hartmann, B.; Lee, G. F.; Lee, J. D. J Acoust Soc Am 1994, 95, 226.
18. Hu, X.; Nawaby, A. V.; Naguib, H. E.; Day, M.; Ueda, K.; Lia, X. Proc Soc Plast Eng Annu Technol Conf 2005, 2670.
19. Chow, T. S. Macromolecules 1980, 13, 362.
20. Chiou, J. S.; Barlow, J. W.; Paul, D. R. J Appl Polym Sci 1985, 30, 2633.
21. Miyata, T.; Masuko, T. Polymer 1998, 39, 5515.
22. Iannace, S.; Nicolais, L. J Appl Polym Sci 1997, 64, 911.